Available online at www.sciencedirect.com
ScienceDirect
Phytochemistry 68 (2007) 2302–2312
PHYTOCHEMISTRY
www.elsevier.com/locate/phytochem

A transient isotopic labeling methodology for ^{13}C metabolic flux analysis of photoautotrophic microorganisms

Avantika A. Shastri, John A. Morgan *

School of Chemical Engineering, Purdue University, 480 Stadium Mall Dr., West Lafayette, IN 47907, USA

Received 16 January 2007; received in revised form 24 March 2007
Available online 23 May 2007

Abstract

Metabolic flux analysis is increasingly recognized as an integral component of systems biology. However, techniques for experimental measurement of system-wide metabolic fluxes in purely photoautotrophic systems (growing on CO_2 as the sole carbon source) have not yet been developed due to the unique problems posed by such systems. In this paper, we demonstrate that an approach that balances positional isotopic distributions *transiently* is the only route to obtaining system-wide metabolic flux maps for purely autotrophic metabolism. The outlined transient ^{13}C-MFA methodology enables measurement of fluxes at a metabolic steady-state, while following changes in ^{13}C-labeling patterns of metabolic intermediates as a function of time, in response to a step-change in ^{13}C-label input. We use mathematical modeling of the transient isotopic labeling patterns of central intermediates to assess various experimental requirements for photoautotrophic MFA. This includes the need for intracellular metabolite concentration measurements and isotopic labeling measurements as a function of time. We also discuss photobioreactor design and operation in order to measure fluxes under precise environmental conditions. The transient MFA technique can be used to measure and compare fluxes under different conditions of light intensity, nitrogen sources or compare strains with various mutations or gene deletions and additions.

Keywords: *Synechocystis* sp. PCC 6803; Transient ^{13}C-MFA; Photosynthesis; Modeling; Calvin cycle; Instationary ^{13}C-MFA

1. Introduction

Metabolic flux analysis (MFA) seeks to quantify the rates of material movement through complex reaction networks (Stephanopoulos et al., 1998). In coordination with information from proteomic, transcriptomic and genomic studies, metabolic flux maps help to decipher the phenotypic outcome of genetic and environmental alterations. The knowledge of the interaction of carbon fixation pathways with other metabolic pathways, under different environmental conditions like light intensity and genetic backgrounds, will increase fundamental biological understanding of photosynthetic metabolism and prove invaluable in modifying photosynthetic systems.

The experimental determination of system-wide metabolic fluxes using ^{13}C tracers (^{13}C-MFA) has been the subject of extensive research in the past decade. It has been successfully applied to study various organisms, such as *Penicillium chrysogenum* (Christensen and Nielsen, 2000), *Escherichia coli* (Fischer and Sauer, 2003; Zhao et al., 2004), various yeasts (Blank et al., 2005), *Bacillus subtilis* (Sauer et al., 1997), *Corynebacterium glutamicum* (Marx et al., 1996), *Synechocystis* (Yang et al., 2002), *Methylobacterium extorquens* (Van Dien et al., 2003), soybean embryos (Sriram et al., 2004) and *Brassica napus* embryos (Schwender et al., 2004). A major strength of ^{13}C-MFA over other modeling approaches (see (Morgan and Rhodes, 2002) for a review in plants) is that complicated kinetic rate equations or enzyme parameter determination are not required for quantification of fluxes through pathways. Information on reversibility of reactions and futile cycles

* Corresponding author. Tel.: +1 765 494 4088; fax: +1 765 494 0805.
E-mail address: jamorgan@purdue.edu (J.A. Morgan).

0031-9422/$ - see front matter © 2007 Elsevier Ltd. All rights reserved.
doi:10.1016/j.phytochem.2007.03.042

that commonly occur in cells can also be partially obtained via ^{13}C-MFA.

^{13}C-MFA is based upon a stoichiometric model of the metabolic system, which involves reconstructing the metabolic network of the organism of interest from genomic and biochemical literature, and writing mass balances around intracellular metabolites (Stephanopoulos et al., 1998). At steady-state, the resultant set of linear algebraic equations is solved to obtain the reaction rates (fluxes). Additional constraints from measured extra-cellular fluxes, such as substrate uptake rates and product secretion rates, aid in solving the internal fluxes (Stephanopoulos et al., 1998). However, in many physiological situations, this set of linear algebraic equations is underdetermined even after all possible external flux measurements are made. This situation has lead to the development of ^{13}C based MFA methods to obtain flux maps (Stephanopoulos et al., 1998; Szyperski, 1998; Wiechert et al., 2001). A flow chart of a typical ^{13}C-MFA process is shown in Fig. 1. In this technique, substrate with carbon labeled at certain positions (^{13}C) is fed to the biological system. Based on the pattern of label incorporation in certain downstream metabolites, indirect information on pathway fluxes is obtained. The labeling patterns are detected by ^{13}C nuclear magnetic resonance (NMR) or mass spectroscopy (MS) (Wiechert et al., 2001). If the fluxes are specified, it is possible to simulate the isotopic labeling patterns. Therefore, the obtained labeling data is used in a constrained non-linear optimization framework, to find the flux distribution that minimizes the difference between simulated and measured labeling patterns. The steady-state mass balances on labeled molecules (isotopomers), the stoichiometric balances and uptake fluxes form the constraints on the problem. Local non-linear optimization techniques (Wiechert et al., 1997), as well as genetic algorithms (Zhao and Shimizu, 2003) have been used to solve the optimization problem.

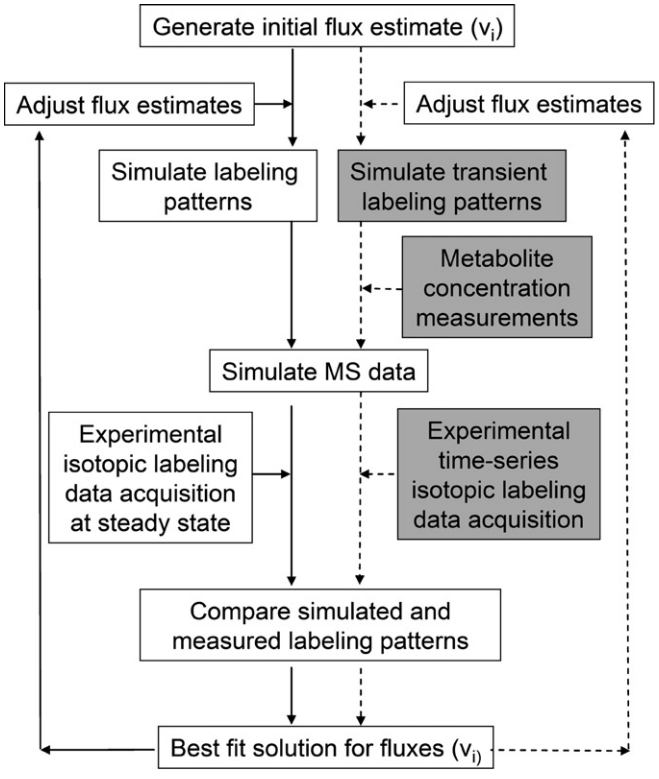

Fig. 1. Flowchart showing the overall schematic of ^{13}C-MFA. Solid arrows show the schematic for steady-state ^{13}C-MFA and dashed arrows show the schematic for the transient ^{13}C-MFA that needs to be applied to photoautotrophic systems that grow on CO_2 as the sole carbon source. The grey boxes highlight the major differences between the two cases.

While the importance of measuring metabolic fluxes in photosynthetic research has been recognized (Fernie et al., 2005; Ratcliffe and Shachar-Hill, 2006; Sweetlove et al., 2003), only a few studies have tried to address the problem of ^{13}C flux analysis in photosynthetic systems; all of these have been under conditions of heterotrophic or mixotrophic growth (Glawischnig et al., 2002; Schwender et al., 2004; Sriram et al., 2004; Yang et al., 2002). It is to be noted that all ^{13}C-MFA techniques currently in practice are at metabolic steady-state with constant fluxes, enzyme levels and metabolite pool sizes. Further, the methods used in most ^{13}C-MFA studies to date are also isotopic steady-state methods, wherein information is obtained after the added isotopic tracer has reached a steady-state labeling pattern within the organism. No studies have applied ^{13}C-MFA to a purely photoautotrophic system (a system with CO_2 as the sole carbon input to the system), since there is a major hurdle, as described below.

In ^{13}C-MFA, the primary information about metabolic fluxes is abstracted from the fact that carbon–carbon bonds of the input are broken and reformed in different, but very specific ways along different metabolic pathways. This is schematically illustrated in Fig. 2 for a heterotrophic system fed on glucose labeled with ^{13}C at position 1 (1-^{13}C). It can be seen that under steady-state conditions, the percentage of ^{13}C in position 1 of the downstream metabolite is influenced by the relative flux through pathway 1 (V_1) over pathway 2 (V_2). In contrast to the heterotrophic case, a photoautotrophic system has CO_2, a one-carbon unit, as the only source of carbon for cell growth (a hypothetical reaction network is shown in Fig. 3(a)). At the start of ^{13}C-labeling experiment ($t = 0$), the feed composition ($^{13}CO_2/^{12}CO_2$ ratio in the feed) is changed to introduce ^{13}C to the system, while keeping the total CO_2 feed rate constant. In such a system, the label accumulates in the system via biochemical reactions, until an isotopic steady-state is reached wherein *all* the carbon atoms in *all* the downstream metabolites are isotopically enriched with ^{13}C to the same extent as the feed, since all the carbons in all the metabolites are ultimately derived from CO_2. This is shown schematically in Fig. 3(b) for a step-change from 100% $^{12}CO_2$ to 100% $^{13}CO_2$. The final labeling steady-state is attained *independent* of the flux distribution. Thus steady-state isotopic ^{13}C-MFA fails to provide any useful information for solving the flux distribution problem.

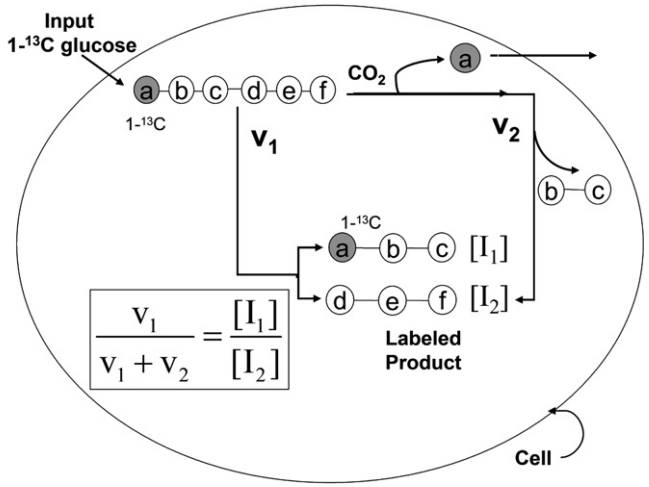

Fig. 2. Schematic of heterotrophic steady-state ^{13}C-MFA with glucose labeling. Gray circles = ^{13}C, white circles = ^{12}C. Pathway 1 leads to formation of both species I_1 and I_2. Pathway 2 loses carbon 'a' and therefore, species I_1 cannot be formed via pathway 2. The relative fluxes through pathways 1 and 2 (V_1 and V_2) can be obtained based on the relative concentrations of species I_1 and I_2 of the downstream products as shown in the equation above. The example is illustrative of steady-state labeling, but for real metabolic networks with cycles and reversible reactions a complete balancing of isotopomers is usually required to quantify fluxes.

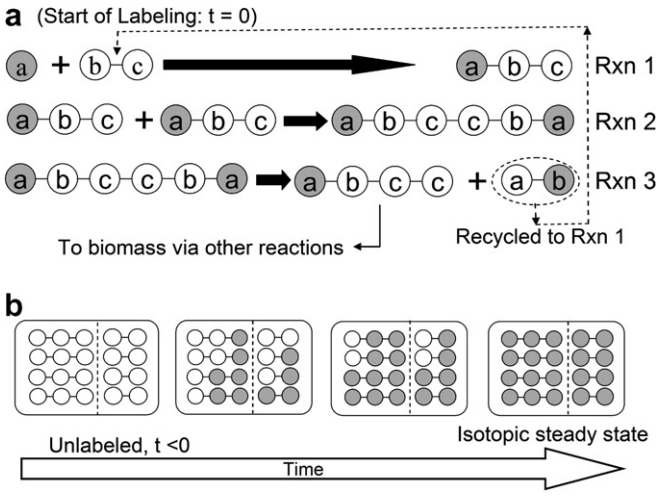

Fig. 3. Schematic of ^{13}C-labeling in photoautotrophic systems. Gray circles = ^{13}C, white circles = ^{12}C, Rxn = reaction. (a) A hypothetical biochemical network showing the fixation of CO_2 into metabolic intermediates of 3, 6, and 4 carbon atoms, via reactions 1, 2, and 3, respectively. A two carbon molecule is recycled back to Rxn 1 from Rxn 3. The reactions show how the label starts propagating in the metabolic network. (b) Time course of labeling, seen in the two and three carbon metabolic intermediates following a step-change to 100% $^{13}CO_2$ at time $t = 0$; At an isotopic steady-state, all molecules downstream of the input CO_2 have carbon atoms labeled to the same extent as the input $^{13}CO_2/^{12}CO_2$ mixture (1:0 in above case), independent of the flux distribution.

However, the *rate* of label enrichment in different isotopomers (as they attain the steady-state value) will depend upon the flux distribution. Therefore, our approach to ^{13}C-MFA in photoautotrophic systems is based on the measurement of *transients* in the isotopomer distribution of metabolites that result from a step change in input ^{13}C (transient ^{13}C-MFA). It is important to note that the method enables the measurement of fluxes at a *metabolic steady-state* (constant metabolic fluxes and internal metabolite concentrations), but utilizes information from transient isotopic data. Furthermore, baring structured kinetic modeling, an approach that balances positional isotopic distributions *transiently* is the only route to obtaining system-wide metabolic flux maps for purely autotrophic metabolism.

Recent improvements in analytical and metabolomic tools, and development of better computational frameworks have facilitated the development of transient ^{13}C-MFA. Wiechert and co-workers have recently extended steady-state ^{13}C-MFA to the transient (instationary) conditions for heterotrophic systems including experimental design (sampling intervals, feed label composition), sensitivity analysis and computational aspects of the transient case (Noh et al., 2006, 2007; Noh and Wiechert, 2006). As expected, the mathematical and computational complexity for the transient case is much greater than the steady-state case (Noh et al., 2007).

In this paper, we outline a methodology to measure steady-state central metabolic fluxes in photoautotrophic systems with a single carbon input, using transient ^{13}C-MFA. Our selected model photosynthetic system, *Synechocystis* sp. PCC 6803, is a fresh water photosynthetic prokaryote, with a fully sequenced genome (Kaneko et al., 1996). It has metabolic pathways of carbon fixation that are similar to higher plants and algae, while possessing a much simpler internal structure due to lack of intracellular compartmentation. It therefore proffers an ideal system to develop ^{13}C-MFA tools for photosynthetic organisms. Starting with the mathematical isotopomer balancing framework, we identify the important aspects of transient labeling in a photosynthetic system, which distinguishes it from steady state MFA. The insights from the modeling framework allow us to delineate the experimental requirements for photoautotrophic ^{13}C-MFA. We also present some interesting practical considerations on bioreactor operation.

2. Results and discussion

2.1. Mathematical framework for transient ^{13}C-MFA

2.1.1. Overall framework

The overall framework of transient ^{13}C-MFA is similar to the steady-state ^{13}C-MFA, but differs in the three key areas, as shown in Fig. 1. These are: (1) isotopic labeling data must be collected as a function of time, (2) the equations to be solved for the forward model are now non-linear differential equations (transient isotopic balances) and (3) intracellular metabolite concentrations also need to be measured. Section 4.1 in the materials and methods

describes the mathematical framework in detail. Eq. 2 (materials and methods) is a transient isotopomer balance equation that describes labeling incorporation in the biochemical network, as a function of time. From Eq. 2, it is clear that the concentrations (pool sizes) of the metabolites impact the observed dynamics, as do the reaction fluxes. It is also clear from this equation that, at isotopic steady-state, the RHS of Eq. 2 equals zero, and hence, the pool sizes play no role in the observed labeling patterns.

The description of the system by isotopomer balances is among the most intuitive, since it describes every single 'physical' ^{13}C labeled species that can be formed. The drawback of using isotopomer balances is that the equations are non-linear differential equations, which can be difficult to solve compared to other approaches given below. Wiechert and co-workers have developed a 'cumomer' framework which transforms the isotopomer framework into a cascade of linear differential equations that must be solved sequentially (Noh et al., 2006), making the system easier to solve than isotopomer balances. Another recent development in representing labeling networks is the 'elementary metabolite unit' or EMU method (Antoniewicz et al., 2007), currently developed for isotopic steady-state MFA. This representation leads to even further reduction of computational complexity. Since some key factors needed to design experiments can readily be deduced from using the isotopomer balances, we have limited ourselves to the isotopomer formulation in this paper.

2.1.2. Transient isotopomer balances in Synechocystis

The forward model for the *Synechocystis* metabolic network was solved using a flux distribution estimate generated by linear programming (see methods). Transient labeling patterns were simulated over a period of 10 min for two different input labeling scenarios, a step-change to 100% ^{13}C, and a step-change to 30% ^{13}C. Figs. 4 and 5 show the mass distribution vectors (MDVs) for selected metabolites for the two cases. An MDV of an *n*-carbon-atom metabolite represents the relative concentrations of the metabolite that contain (0, 1, 2, …, *n*) ^{13}C atoms (mass isotopomers). Since MDVs are often directly measurable by MS, it is informative to plot simulated MDV data instead of simulated isotopomer data. For the 100% step-change, we see a shift from the completely unlabeled to the fully labeled molecules for all the metabolites, while traversing through all intermediate mass isotopomers, as can be expected. Metabolite pools closer to the carbon fixation reactions get labeled faster than molecules far downstream (3-phosphoglycerate versus α-ketoglutarate). Compared to the 30% labeling case, the observed transients are more dramatic for the 100% step-change, with the relative concentration of each mass isotopomer reaching a significant (measurable) level at some point of time during the experiment. In contrast, for the 30% labeling case, the higher mass isotopomers do not reach high concentrations, and may not be detectable by MS. The optimal labeling strategy should therefore involve utilization of the highest percentage of labeling that is practically feasible.

The simulation of the forward model is useful to design a timeframe for the labeling experiment. From Figs. 4 and 5, we see that the simulated transients occur over a period of 10 min. We must caution that, there are potential errors in this estimated time frame, since the fluxes used did not include any reversible fluxes. This shortcoming is inherent

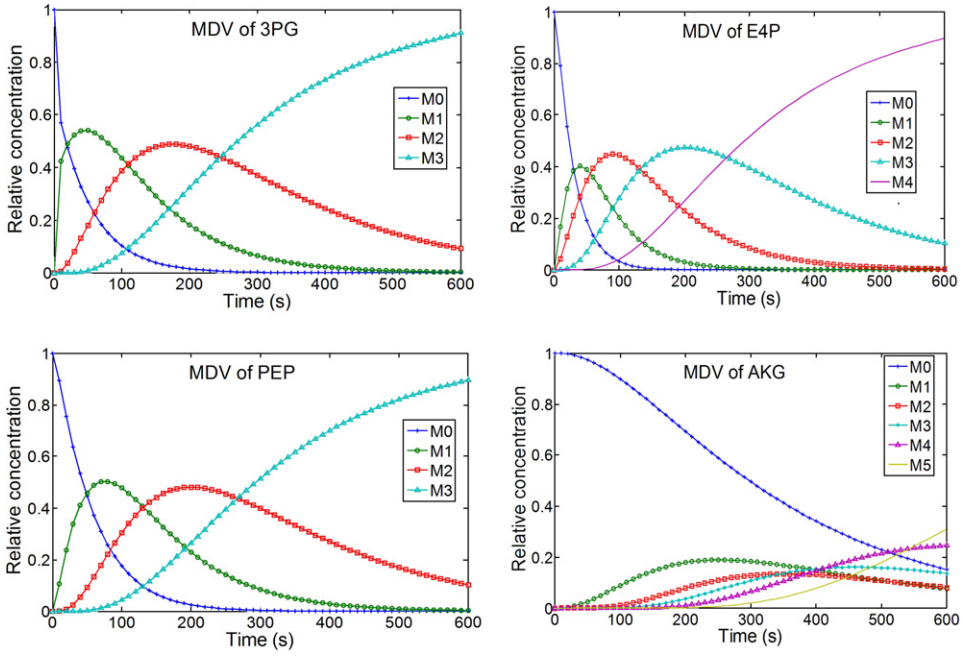

Fig. 4. Mass distribution vectors (MDV) of selected intermediates in response to a carbon dioxide step-change from 0% to 100% ^{13}C. 3PG = 3-phosphoglycerate, E4P = erythrose 4-phosphate, PEP = phosphoenol pyruvate, AKG = α-ketoglutarate. *Mi* = fraction of the total metabolite pool containing *i* number of labeled carbons.

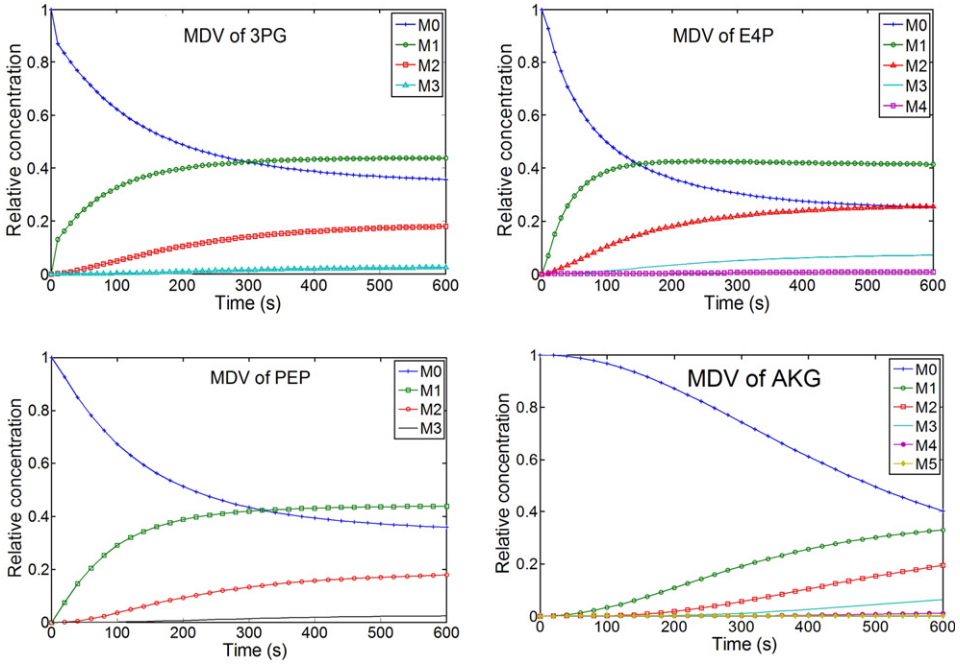

Fig. 5. Mass distribution vectors (MDV) of selected intermediates in response to a carbon dioxide step-change from 0% to 30% ^{13}C. 3PG = 3-phosphoglycerate, E4P = erythrose 4-phosphate, PEP = phosphoenol pyruvate, AKG = α-ketoglutarate. *Mi* = fraction of the total metabolite pool that contain *i* number of labeled carbons.

to the stoichiometric approach used to estimate the fluxes (Shastri and Morgan, 2005). However, in the absence of any available flux measurement data for the photoautotrophic case, it still provides us with reasonable estimate for an initial experiment. An analysis of the effect of ignoring reversible fluxes shows that the forward flux through a reversible reaction will exceed the net flux (calculated by linear programming), thereby increasing the rate of labeling dynamics. If the degree of reversibility is very high, the timescale of the entire labeling process could decrease by an order of magnitude (1 min instead of 10 min). However, the time scale can be further refined based upon the labeling rates seen in the first 10 min experiment. In order to capture the maximum labeling dynamics, an ideal experimental setup should facilitate withdrawal of several samples within few minutes. Further, each sample should be withdrawn and quenched in the sub-second time scale. Wiechert and co-workers advocate the rapid withdrawal of more samples than may actually be used, with an *a posteriori* selection of samples to analyze, based upon concentration measurement data (Noh and Wiechert, 2006). The selection is made to maximize the statistical quality of estimated parameters (fluxes).

2.2. Experimental design

2.2.1. Choice of measured metabolic intermediates

In most of the steady-state ^{13}C-MFA studies, proteinogenic amino acids are the choice of metabolites measured, by virtue of being in high cellular concentration and deriving from all parts of central metabolism. As stated earlier, concentration measurements are a necessary part of the transient isotopic method. If the measured metabolites of choice are proteinogenic amino acids, or even soluble amino acids, the pool size (and labeling patterns) of every intermediate leading up to the amino acids/proteins should be modeled and measured. In order to restrict the size of the model and number of measured intermediates in an already difficult problem, the best metabolites to measure are not the amino acids but the central carbon intermediates themselves. While overcoming problems posed by proteinogenic amino acids, they have the drawback of being present in much lower intracellular concentrations, thereby requiring larger sample sizes for analysis.

2.2.2. Metabolite concentrations and transient isotopic data acquisition

Steady-state MFA procedures utilize both NMR and mass spectroscopy for the determination of labeling patterns (Wiechert et al., 2001). While NMR provides direct information about each labeled ^{13}C–^{13}C bond within a molecule, MS data can only provide partial information about labeled positions. However, MS methods have significantly greater sensitivities (several orders of magnitude) than ^{13}C NMR. This consideration tends to outweigh its drawbacks, and it is increasingly the method of choice in the field of ^{13}C-MFA (Noh and Wiechert, 2006; van Winden et al., 2005). Since transient ^{13}C-MFA requires several samples to be taken over a short period of time, it enforces further restrictions on the size of each sample, and hence requires MS methods of isotopomer analysis.

Table 1
Concentrations of some key central metabolites in *Synechocystis* measured by GC–MS

Intracellular metabolite	Pool size, μmol/g dry wt.	r^2 value of calibration
3-Phosphoglycerate	6	0.985
α-Ketoglutarate	2	0.983
Fructose 6-phosphate	5	0.954
Fumarate	9	0.979
Glucose 6-phosphate	2	0.954
Isocitrate	5	0.985
Malate	4	0.987
Phosphoenol pyruvate	4	0.984
Ribulose 1,5-bisphosphate	10	0.863
Ribulose 5-phosphate	3	0.984
Succinate	4	0.985

The values were used to simulate the forward model. A dry weight of 7 mg biomass was used for the measurements.

For the analysis of central carbon intermediates, the vast majority of the metabolites are characterized by the presence of carboxylic acid or phosphate groups, which necessitates the use of derivatization agents for GC–MS analysis (Roessner et al., 2000). We obtained estimates of the concentrations of several central intermediates (see Table 1) from a *Synechocystis* culture grown in shake flasks using GC–MS (see materials and methods). These concentrations were used as parameters in the forward model. However, some caution is needed while using GC–MS based techniques for metabolite quantification. It has recently been shown that different metabolites are derivatized at different rates, and the differences are amplified when there are multiple functional groups on a molecule (Kanani and Klapa, 2007). Furthermore, the intermediates as well as final products are also subject to degradation. One approach to overcome these problems is by the automation of derivatization and sample injection, whereby each sample is derivatized for the same time before analysis on the GC–MS. Alternately, application of data correction strategies can take these differences into account (Kanani and Klapa, 2007). We are currently investigating the effects of derivatization time on the central metabolic intermediates.

The presence of phosphate and carboxylic acid groups also make the central carbon metabolites amenable to analysis by LC or CE–MS. Two different LC–MS methods, a graphite column based method (Buchholz et al., 2001) and an ion-exchange method (van Dam et al., 2002), have been used to analyze metabolite concentrations. They have reported injection volumes of 10–20 μL, with detection limits in the range of 3–21 μM and 14–140 μM, respectively. A third LC–MS method using an amino column has recently been reported to characterize intracellular metabolite concentrations (Bajad et al., 2006). The typical detection limits from this method are in the range of 0.29–8.8 μM for most central metabolites of interest, due to a narrower column bore. Since most central intermediates are found in concentration ranges of 10^{-2} to 10 μmol/g dry weight, typical biomass sample size required for quantification is in the range of 1–10 mg of dry cell weight. We have found typical *Synechocystis* cell densities in a chemostat growth rate 0.04 h^{-1}, 350 μE/m^2/s average surface light flux, and enhanced CO_2 feed are approximately 350 mg/L. Under such conditions, minimum sample sizes required are on the order of 3–30 mL per sample. Clearly, any improvements in sensitivity of analytical techniques will tremendously aid in practical realization of photoautotrophic MFA. CE–MS is yet another promising technique for use in metabolite concentration measurements (Sato et al., 2004; Soga et al., 2002) and isotopic labeling measurements. For example, CE/MS was recently used to measure labeling patterns in amino acids in a steady-state ^{13}C-MFA study on *E. coli* (Iwatani et al., 2007). The detection limits (in the range of 0.3–6.7 μM) are at least two orders of magnitude lower than LC–MS methods (Soga et al., 2002). Unlike GC–MS, this method does not require derivatization. Therefore, it has some advantages over current GC (simpler sample preparation) as well as LC methods (detection limits).

2.2.3. Rapid sampling and bioreactor configuration

Obtaining samples for metabolic concentration and isotopic distribution measurements from the biological reactor involves three important phases: removing sample from the system, rapid quenching of metabolism and extraction of metabolites from the sample. Typically, the first two phases are combined into a single step (Larsson and Tornkvist, 1996; Schaefer et al., 1999; Visser et al., 2002), although there are schemes that combine all three into a single step (Schaub et al., 2006). From the results in Section 2.1.2, it is evident that transient ^{13}C-MFA requires several samples to be taken over a very short period of time. The time scale of the transients could vary from a few seconds to a few minutes, depending upon both the fluxes and pool sizes. Any experimental design scheme must therefore include withdrawal and quenching of samples from a bioreactor, while allowing for several samples to be obtained in quick succession. There are several rapid sampling schemes that have been designed to obtain samples in the sub-second to seconds timeframe (Lange et al., 2001; Theobald et al., 1993; Visser et al., 2002). Several methods of quenching including cold shocks (Buziol et al., 2002; Schaefer et al., 1999; Visser et al., 2002) and heat treatment (Villas-Boas et al., 2005) have been investigated by researchers. A considerable problem is faced when quenching is accompanied by intracellular metabolite leakage into the quench solution (Villas-Boas et al., 2005; Wittmann et al., 2004), and the optimal quenching method needs to be identified for every organism. When quenching and extraction are carried out in a single step, the volume of each sample to be processed (concentrated) increases several fold. Further, the sample will retain a significant proportion of salts, buffers and other media components which can cause complex matrix effects when the sample

is analyzed by LC–MS. As yet, there is no single quenching procedure that has clear advantages over other methods. It is important to note that the total concentration of each labeled pool is assumed (more specifically, required) to be constant over the experiment. Therefore, only a single measurement (data point) is needed to obtain absolute concentration of pool sizes. This data point can be obtained before the start of the labeling step-change while the remaining samples only need to be analyzed for isotopic label enrichment.

Synechocystis (and many other cyanobacteria) can uptake and utilize both CO_2 and HCO_3^- via several different transporters and carbon uptake systems, that are activated under various physiological conditions of carbon and light availability (Badger et al., 2006). The supply of carbon to a culture of *Synechocystis* therefore forms a very critical aspect of the experimental design. For a chemostat culture, cells can be fed either labeled CO_2 through aeration or labeled bicarbonate in the liquid media. Under physiological pH conditions for *Synechocystis* (6.8–9), carbonate concentrations in water are negligible compared to bicarbonate and dissolved CO_2 concentrations. Hence, CO_3^{2-} will be omitted from the following discussion.

For carbon limited cultures, the residual carbon concentration in the reactor will be close to zero. Thus, all entering carbon will be rapidly consumed by the culture. A step-change from unlabeled to labeled carbon can therefore be made nearly instantaneous. However, in the case of light limited cultures, the dissolved CO_2 concentration (or total dissolved carbon dioxide and bicarbonate concentration, C_{total}) in the reactor is expected to be high, in order to ensure that light is the limiting factor. When CO_2 is fed to the system, the residence time of C_{total} in the reactor is determined by a combination of the volumetric gas–liquid mass transfer coefficient, k_la, carbon consumption rate, and dilution rate (media flow rate/reactor volume). The composition of air fed (% CO_2 in air) to the system, is another important design parameter in photobioreactor operation, and enhanced (>0.03%) CO_2 is often used in order to enhance the mass transfer rate. The effect of these parameters can be analyzed using Eqs. (7)–(9) (see materials and methods). Results for a typical bioreactor condition (cell density 350 mg/L, 0.5 kg C assimilated/kg biomass formed, $\mu = 0.04\ h^{-1}$) are discussed here. Fig. 6 shows the effect of k_la on the dynamics of ^{13}C replacing ^{12}C in the reactor following a step-change. The graph shows that increasing k_la leads to longer lag times before the steady-state concentration of $^{13}C_{total}$ is attained. Fig. 7 shows the effect of feed CO_2 content (% CO_2 in air), at a k_la value of $0.014\ s^{-1}$. It is clear that as the percentage of CO_2 in the feed increases, it takes longer to replace all of the ^{12}C with ^{13}C. These trends are due to the fact that increased k_la and increased CO_2 percentage, both cause an increase in the total dissolved carbon content of the reactor. The process of slow replacement of ^{12}C by ^{13}C obviously affects the observed labeling dynamics of intracellular metabolites. Thus, light limited studies should be designed to keep the

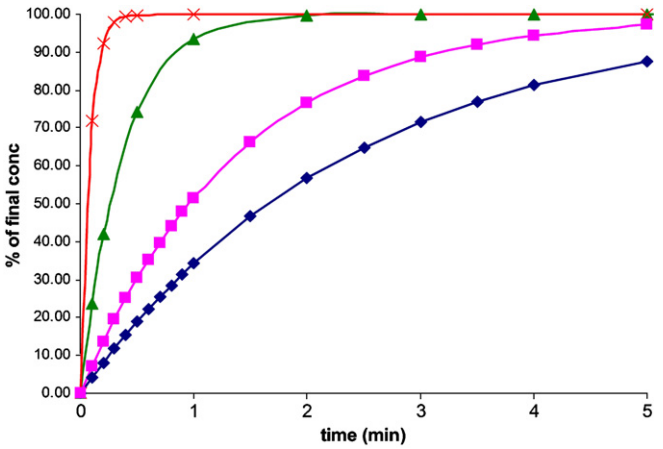

Fig. 6. Effect of k_la on the dynamics of $^{13}CO_2$ following a step-change in feed from 0% to 100% $^{13}CO_2$. ◆ = $0.03\ s^{-1}$, ■ = $0.02\ s^{-1}$, ▲ = $0.015\ s^{-1}$ and × = $0.014\ s^{-1}$.

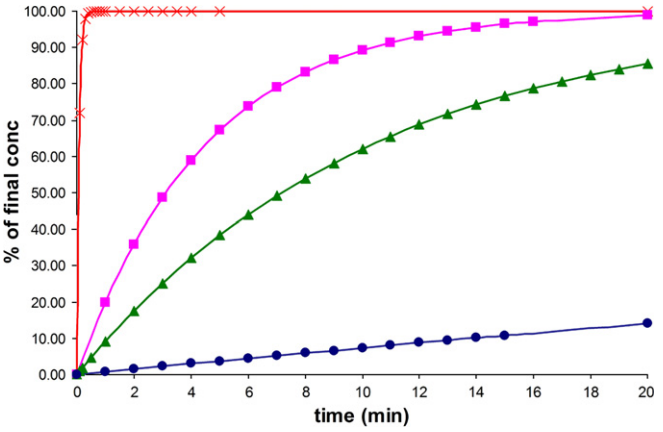

Fig. 7. Effect of the percentage of CO_2 in air on the dynamics of $^{13}CO_2$ following a step-change in feed from 0% to 100% $^{13}CO_2$. ● = 1%, ▲ = 0.1%, ■ = 0.06% and × = 0.03%.

total dissolved carbon concentration as low as possible without switching into CO_2 limited regimes. If it is not possible to select operating conditions that result in a rapid step-change in the feed, the dynamics of $^{13}C/^{12}C$ ratio in the reactor as a function of time will also have to be simulated in order to calculate fluxes. In order to circumvent these problems, it is possible to use labeled bicarbonate feed through liquid media instead of CO_2. In this case, as in the case of CO_2 feeding, C_{total} is likely to be large. Therefore, merely replacing $H^{12}CO_3^-$ is by $H^{13}CO_3^-$ in the liquid media will cause the ^{12}C replacement dynamics to be governed by dilution rate (on the order of hours). Thus, a significantly rapid replacement of $^{12}C_{total}$ will be possible only if a large quantity of $H^{13}CO_3^-$ is pulsed into the reactor at the start of the labeling experiment. For example, adding an amount of $H^{13}CO_3^-$ equal to half the amount of $H^{12}CO_3^-$ already existing in the reactor, leads to a 33% labeling experiment. Obtaining higher labeling percentages will require adding even larger amounts of $H^{13}CO_3^-$.

Although a rapid step-change can be obtained in this manner, it may not be possible to obtain a very high labeling percentage, since a large excess of bicarbonate may cause significant physiological changes in the organism.

Growing photosynthetic microbes at steady-state in a chemostat allows the growth rate to be controlled (by setting media flow rate), but it does not give independent control over light intensity per cell, since the average light intensity inside the reactor is affected by culture density. Thus, in order to study the effect of light intensity on fluxes, or compare flux maps while holding light intensity per cell as constant, a turbidostat is a superior choice. A turbidostat is a bioreactor where the cell density of a culture is kept constant, enabling the control of average light flux incident per cell.

3. Concluding remarks

In this paper, we presented an overview of a ^{13}C-MFA methodology for microorganisms growing on CO_2 as the sole carbon source. The methodology utilizes transient labeling data to calculate central metabolic fluxes. In order to apply ^{13}C-MFA to photosynthetic microbes, one significant technical hurdle is growing cells autotrophically to a high cell density under physiologically relevant CO_2 concentrations. This requires a photobioreactor design that can provide uniform light supply (to prevent cell-shading) and good mixing at the same time (to provide a rapid step change of ^{13}C). Furthermore, it must be equipped with a suitable rapid sampling device, preferably automated. Due to very recent developments in the field (Antoniewicz et al., 2007; Noh and Wiechert, 2006), there are no longer any major computational hurdles. Rapid progress of metabolomic techniques (extraction and separation techniques for MS) is helping to overcome many of the experimental challenges with obtaining large enough sample sizes. We believe that within a year the technique can be satisfactorily applied to *Synechocystis* under some specific growth conditions. Since the fluxes are measured by following labeling patterns in low concentration primary metabolites, further increases in the sensitivity of MS based analytical techniques are required in order to apply the method to a wide range of growth conditions. Once established, this technique will enable studies of central metabolic fluxes under various environmental conditions and genetic backgrounds. Coupled with other 'omics' based approaches, it will allow a deeper understanding of how the combination of genes and enzymes manifest themselves as a working photosynthetic metabolic system.

4. Methods

4.1. Modeling framework for ^{13}C-MFA

The detailed modeling framework for (metabolic) steady-state ^{13}C-MFA has been developed by several competing researchers (Park et al., 1999; Szyperski, 1998; Wiechert et al., 2001). The general transient ^{13}C-MFA framework (Noh et al., 2006), based on the steady-state case, with suitable modifications, is presented below for *Synechocystis*.

4.1.1. Stoichiometric model of the Synechocystis reaction network

The central metabolic pathways of *Synechocystis* were annotated from its genomic data (Kaneko et al., 1996). The reconstructed reaction network consists of 76 reactions and 37 metabolites (Shastri and Morgan, 2005). Reversible reactions were divided into forward and reverse fluxes. Reactions were defined to be of three types, uni (one reactant, one product), uni–bi (one reactant, two products), and bi–uni (two reactants, one product). Reactions of the type bi–bi (two reactants, one product) were split into two reactions, a bi–uni and a uni–bi, with a fictitious unimolecular intermediate (Wiechert et al., 1999). These are the 2C, 3C and 6C intermediates that arise in the Calvin cycle and pentose phosphate pathway (Supplementary Table 1). The biomass formation equation was formulated based on biomass composition measurements made on mid-exponential phase batch cultures of *Synechocystis* (Shastri and Morgan, 2005). At a metabolic steady-state, mass balances written around intracellular intermediates lead to a system of linear algebraic equations represented by:

$$S \cdot v = 0 \tag{1}$$

where S is the stoichiometric matrix, and v is a vector of (unknown) fluxes.

4.1.2. Transient ^{13}C-label balancing

In order to track the path of a ^{13}C pulse (or step-change) through the metabolic network, the carbon atom transitions in each reaction are described using atom mapping matrices (AMMs) (Stephanopoulos et al., 1998). In this model, isotopomers are used as the fundamental physical unit of a ^{13}C-labeled molecule. The rate of accumulation of label in various isotopomers can be described by a mass balance equation, in matrix–vector form as (Wiechert et al., 1999):

$$\frac{\mathrm{d}(\mathbf{CI})}{\mathrm{d}t} = \sum_{j=1}^{n} v_j \mathbf{P}_j \mathbf{I} + 0.5 \sum_{j=1}^{n} \mathbf{I}^{\mathrm{T}} v_j \mathbf{Q}_j \mathbf{I} + \sum_{\mathrm{inp}=1}^{\mathrm{ninp}} v_{\mathrm{inp}} \mathbf{P}_{\mathrm{inp}} \mathbf{I}_{\mathrm{inp}} \tag{2}$$

where $\mathbf{I}$ is the overall isotopomer distribution vector, $\mathbf{P}_j$ is a matrix describing the transitions from reactant to product isotopomers for the jth internal metabolic reaction containing a single reactant, $\mathbf{Q}_j$ is a matrix describing the transitions from reactant to product isotopomers for the jth internal metabolic reaction involving two reactants and a single product, and v_j is the flux of the jth reaction. $\mathbf{C}$ is a diagonal matrix corresponding to intracellular metabolite concentrations. $\mathbf{P}_{\mathrm{inp}}$ is a matrix describing transitions from extra-cellular reactants (input) to their intracellular

counterparts. $\mathbf{I}_{inp}$ is the isotopomer distribution vector of the input reactants and v_{inp} is the input flux vector. n and ninp are the total number of internal and input reactions, respectively. Unlike the case of steady-state labeling methods, where Eq. (2) equals zero, the concentrations of metabolites do not drop out of the equation. Therefore, concentration measurements form a necessary part of the transient isotopic method. Eq. (2) is a set of non-linear ordinary differential equations, which can be solved numerically, if the values of concentrations and fluxes are specified. This is termed as 'solving the forward model'.

MATLAB v. 7.01 (MathWorks, Natick, MA) was used to define AMMs for the model listed in Supplementary Table 2. Scripts were written to generate the P and Q matrices from the defined AMMs and metabolites. A flux distribution was generated from previous work, using linear programming to maximize biomass flux, while minimizing light utilization (Shastri and Morgan, 2005). The flux values are listed in Supplementary Table 2. Several metabolite pool sizes were measured using GC–MS (Table 1) for a sample of *Synechocystis* to obtain realistic orders of magnitude estimates of intracellular concentrations (see below for growth conditions of *Synechocystis*). For the remaining unmeasured metabolites, pool sizes were assumed to be an order of magnitude lower than the measured pools (0.1 μmol/g dry wt.). Pool sizes were assumed to be two orders of magnitude lower for the fictitious metabolites (0.01 μmol/g dry wt.), since these are metabolites that are not actually present, but are required to represent bi–bi type reactions (Wiechert et al., 1999). Metabolite pool sizes used in the model are listed in Supplementary Table 1. The specific cell growth rate was assumed to be 0.04 h^{-1}, which is approximately half the maximum growth rate of *Synechocystis* (Shastri and Morgan, 2005). Using the reconstructed network, flux estimates and pool sizes, Eq. (2) was solved numerically using the ode23 solver in MATLAB v. 7.01 (MathWorks, Natick, MA).

4.1.3. Optimization framework for solving unknown fluxes

In order to quantify the fluxes, v_j, an optimization problem is formulated, which minimizes the error between measured labeling patterns and those predicted by Eq. (2). The differential equations described by Eq. (2), and the stoichiometric model described by Eq. (1) form the constraints of the optimization. The formal statement of the problem is described as follows:

$$\text{minimize}(\text{MDV}_{meas} - \text{MDV}_{calc})^2 \tag{3}$$

$$\text{subject to } S \cdot v = 0 \tag{1}$$

$$\frac{d(\mathbf{CI})}{dt} = \sum_{j=1}^{n} v_j \mathbf{P}_j \mathbf{I} + 0.5 \sum_{j=1}^{n} \mathbf{I}^T v_j \mathbf{Q}_j \mathbf{I} + \sum_{inp=1}^{ninp} v_{inp} \mathbf{P}_{inp} \mathbf{I}_{inp} \tag{2}$$

$$\text{MDV}_{calc} = \mathbf{M}_{IDV-MDV}\mathbf{I} \tag{4}$$

$$v_{bm} = \mu Y \tag{5}$$

$$v_{inp\_CO_2} = 100 \tag{6}$$

where, $\mathbf{M}_{IDV-MDV}$ is a matrix that converts the isotopomer distribution vector ($\mathbf{I}$) into the calculated mass distribution vector (MDV_{calc}), and MDV_{meas} is the measured mass distribution vector of all the intermediates at all time points. An MDV of an n-carbon-atom metabolite is a vector of $(n+1)$ mass fractions, that represent the relative concentrations of molecules that contain $(0, 1, 2, \ldots, n)$ ^{13}C atoms. The basis of the calculation is normalized to a carbon dioxide input (v_{inp_CO2}) of 100 μmol h^{-1}, μ is the specific growth rate (h^{-1}), v_{bm} is the flux to biomass, and Y the biomass yield per 100 μmol of CO_2 fixed by the system. Un-measurable pool sizes can also be included as unknown parameters in the problem.

4.2. Synechocystis growth conditions

Synechocystis sp. PCC 6803 was obtained from ATCC (ATCC # 27150), and grown at 30 °C in 50 mL shake flask cultures with shaking at 300 rpm, a surface light flux of 20–30 uE/m^2/s, in BG-11 medium (ATCC medium 616) buffered with 10 mM HEPES under atmospheric levels of carbon dioxide (0.03%). Growth was monitored spectrophotometrically by measuring the optical absorbance of cultures at 730 nm. A correlation of 0.3 g dry wt./L/OD_{730nm} was used to calculate cell density. Bioreactor runs were performed in a 1.25 L bioreactor (Bioflo 3000, New Brunswick Scientific, NJ), with temperature and pH control. Nine 23 W cool white fluorescent lights (Sylvania, MA) were used to provide light flux to the reactor.

4.3. Metabolite quenching and extraction

A modified cold methanol quenching (van Dam et al., 2002) followed by a modified cold methanol extraction procedure (Maharjan and Ferenci, 2003) was used to obtain samples for GC–MS. *Synechocystis* shake flask samples were quenched with equal volumes of 60% methanol–water solution at −50 °C. The quenched solution was centrifuged for 10 min at 8000 g at −20 °C. The supernatant was discarded and the cell pellet was extracted with 500 μL pure methanol, followed by two extractions with 500 μL 50% methanol–water solution. Each extraction was carried out for 30 min, and the extracts were pooled together and stored at −20 °C.

4.4. GC–MS for metabolite concentration measurements

The GC–MS method was adapted from (Roessner et al., 2000). All samples (standards and biomass extracts) were dried under vacuum, at room temperature, in a Centrivap (Labconco Corporation, MO). Ribitol was added as an internal standard to all the samples, prior to the drying step so as to achieve a final concentration of 0.328 μM in the derivatized solution. The samples were subsequently methoximated with 50 (or 100) μL of methoxyamine hydrochloride in pyridine (2 mg/mL) for 90 min at 40 °C.

This reaction protects carbonyl carbons, and prevents the formation of multiple TMS derivatives (Roessner et al., 2000). Next, 50 (or 100) μl of BSTFA + 10% TMCS (Pierce Biotechnology, IL) was added to the reaction mixture, and incubated at 40 °C for 30 min. The derivatized samples remained for 6–12 h at room temperature, in a dessicator, to ensure complete reaction. All samples were run on the GC–MS within 30 h of derivatization. A Pegasus TOF Mass Spectrometer (LECO Corporation, MI) with a 180 μm diameter, 10 m length, and 0.20 μm film thickness DB-5 column (Agilent Technologies Inc, CA) was used with helium as the carrier gas. The total column flow was set to 1 ml/min, with 260 °C inlet temperature and a split ratio of 1:25. The temperature was held at 70 °C for 5 min, increased to 300 °C at a 5 °C/min, and held at 300 °C for 1 min. The column was equilibrated for 1 min at 70 °C between runs. Linear calibration curves were prepared with purchased standards and used to quantify the metabolites in the samples. Metabolites were identified by comparison of retention time and characteristic ions with standards. All chemicals were purchased from Sigma Aldrich, USA.

4.5. Carbon balances on a chemostat

In aqueous solution, CO_2 exists as three different species, dissolved CO_2, HCO_3^-, and CO_3^{2-}. The pH has a profound effect on the relative concentrations of the three species. Assuming equilibrium between the three species and assuming dissolved CO_2 is in equilibrium with the gas phase CO_2 concentration, the total carbon balance on the chemostat can be written as:

$$k_l a(C^* - C_{CO_2}) - DC_{CO_2}\left\{1 + \frac{K_1}{[H^+]} + \frac{K_1K_2}{[H^+]^2}\right\} - R = 0 \quad (7)$$

where D is the dilution rate, (time^{-1}), C_{CO_2} is the dissolved CO_2 concentration, C^* is the saturation concentration of CO_2 in liquid phase, as determined by Henry's law, K_1 and K_2 are the first and second equilibrium constants between CO_2, HCO_3^-, and CO_3^2, $k_l a$ is the volumetric mass transfer coefficient (time^{-1}), R is the rate of carbon assimilation into biomass (mol C/volume/time). $[H^+]$ is calculated from knowledge of pH, and C_{CO_2} can be calculated from Eq. (7). Further, the total dissolved carbon content, C_{total} (sum of dissolved CO_2, bicarbonate and carbonate), can be calculated from C_{CO_2} as follows:

$$C_{total} = C_{CO_2}\left\{1 + \frac{K_1}{[H^+]} + \frac{K_1K_2}{[H^+]^2}\right\} \quad (8)$$

A mass balance on total dissolved ^{13}C, to simulate the replacement of total ^{12}C in the reactor with ^{13}C, (assuming CO_2 feeding through aeration) is given by:

$$\frac{d^{13}C_{total}}{dt} = k_l a(C^* - C_{CO_2}) - D^{13}C_{total} - R\frac{^{13}C_{total}}{C_{total}} \quad (9)$$

where $^{13}C_{total}$ is the total dissolved ^{13}C concentration in the media (sum of dissolved $^{13}CO_2$, $^{13}HCO_3^-$ and $^{13}CO_3^{2-}$). Eq. (9) can be integrated to obtain $^{13}C_{total}$ as a function of time.

Acknowledgements

This work was funded by the National Science Foundation (BES 0348458) and the National Institutes of Health (R33 DK070290-03).

Appendix A. Supplementary material

Supplementary data associated with this article can be found, in the online version, at doi:10.1016/j.phytochem.2007.03.042.

References

Antoniewicz, M.R., Kelleher, J.K., Stephanopoulos, G., 2007. Elementary metabolite units (EMU): a novel framework for modeling isotopic distributions. Metabol. Eng. 9, 68–86.

Badger, M.R., Price, G.D., Long, B.M., Woodger, F.J., 2006. The environmental plasticity and ecological genomics of the cyanobacterial CO_2 concentrating mechanism. J. Exp. Bot. 7, 249–265.

Bajad, S.U., Lu, W.Y., Kimball, E.H., Yuan, J., Peterson, C., Rabinowitz, J.D., 2006. Separation and quantitation of water soluble cellular metabolites by hydrophilic interaction chromatography–tandem mass spectrometry. J. Chromatogr. A 1125, 76–88.

Blank, L.M., Lehmbeck, F., Sauer, U., 2005. Metabolic-flux and network analysis in fourteen hemiascomycetous yeasts. FEMS Yeast Res. 5, 545–558.

Buchholz, A., Takors, R., Wandrey, C., 2001. Quantification of intracellular metabolites in *Escherichia coli* K12 using liquid chromatographic–electrospray ionization tandem mass spectrometric techniques. Anal. Biochem. 295, 129–137.

Buziol, S., Bashir, I., Baumeister, A., Claassen, W., Noisommit-Rizzi, N., Mailinger, W., Reuss, M., 2002. New bioreactor-coupled rapid stopped-flow sampling technique for measurements of metabolite dynamics on a sub-second time scale. Biotechnol. Bioeng. 80, 632–636.

Christensen, B., Nielsen, J., 2000. Metabolic network analysis of *Penicillium chrysogenum* using ^{13}C-labeled glucose. Biotechnol. Bioeng. 68, 652–659.

Fernie, A.R., Geigenberger, P., Stitt, M., 2005. Flux an important, but neglected, component of functional genomics. Curr. Opin. Plant Biol. 8, 174–182.

Fischer, E., Sauer, U., 2003. Metabolic flux profiling of *Escherichia coli* mutants in central carbon metabolism using GC–MS. Eur. J. Biochem. 270, 880–891.

Glawischnig, E., Gierl, A., Tomas, A., Bacher, A., Eisenreich, W., 2002. Starch biosynthesis and intermediary metabolism in maize kernels. Quantitative analysis of metabolite flux by nuclear magnetic resonance. Plant Physiol. 130, 1717–1727.

Iwatani, S., Van Dien, S., Shimbo, K., Kubota, K., Kageyama, N., Iwahata, D., Miyano, H., Hirayama, K., Usuda, Y., Shimizu, K., Matsui, K., 2007. Determination of metabolic flux changes during fed-batch cultivation from measurements of intracellular amino acids by LC–MS/MS. J. Biotechnol. 128, 93–111.

Kanani, H.H., Klapa, M.I., 2007. Data correction strategy for metabolomics analysis using gas chromatography–mass spectrometry. Metabol. Eng. 9, 39–51.

Kaneko, T., Sato, S., Kotani, H., Tanaka, A., Asamizu, E., Nakamura, Y., Miyajima, N., Hirosawa, M., Sugiura, M., Sasamoto, S., Kimura, T., Hosouchi, T., Matsuno, A., Muraki, A., Nakazaki, N., Naruo, K., Okumura, S., Shimpo, S., Takeuchi, C., Wada, T., Watanabe, A., Yamada, M., Yasuda, M., Tabata, S., 1996. Sequence analysis of the genome of the unicellular cyanobacterium *Synechocystis* sp. strain PCC 6803. II. Sequence determination of the entire genome and assignment of potential protein-coding regions. DNA Res. 3, 109–136.

Lange, H.C., Eman, M., van Zuijlen, G., Visser, D., van Dam, J.C., Frank, J., de Mattos, M.J.T., Heijnen, J.J., 2001. Improved rapid sampling for in vivo kinetics of intracellular metabolites in *Saccharomyces cerevisiae*. Biotechnol. Bioeng. 75, 406–415.

Larsson, G., Tornkvist, M., 1996. Rapid sampling, cell inactivation and evaluation of low extra-cellular glucose concentrations during fed-batch cultivation. J. Biotechnol. 49, 69–82.

Maharjan, R.P., Ferenci, T., 2003. Global metabolite analysis: the influence of extraction methodology on metabolome profiles of *Escherichia coli*. Anal. Biochem. 313, 145–154.

Marx, A., de Graaf, A.A., Wiechert, W., Eggeling, L., Sahm, H., 1996. Determination of the fluxes in the central metabolism of *Corynebacterium glutamicum* by nuclear magnetic resonance spectroscopy combined with metabolite balancing. Biotechnol. Bioeng. 49, 111–129.

Morgan, J.A., Rhodes, D., 2002. Mathematical modeling of plant metabolic pathways. Metabol. Eng. 4, 80–89.

Noh, K., Gronke, K., Luo, B., Takors, R., Oldiges, M., Wiechert, W., 2007. Metabolic flux analysis at ultra short time scale: isotopically non stationary ^{13}C-labeling experiments. J. Biotechnol. 129, 249–267.

Noh, K., Wahl, A., Wiechert, W., 2006. Computational tools for isotopically instationary ^{13}C-labeling experiments under metabolic steady-state conditions. Metabol. Eng. 8, 554–577.

Noh, K., Wiechert, W., 2006. Experimental design principles for isotopically instationary ^{13}C-labeling experiments. Biotechnol. Bioeng. 94, 234–251.

Park, S.M., Klapa, M.I., Sinskey, A.J., Stephanopoulos, G., 1999. Metabolite and isotopomer balancing in the analysis of metabolic cycles: II. Applications. Biotechnol. Bioeng. 62, 392–401.

Ratcliffe, R.G., Shachar-Hill, Y., 2006. Measuring multiple fluxes through plant metabolic networks. Plant J. 45, 490–511.

Roessner, U., Wagner, C., Kopka, J., Trethewey, R.N., Willmitzer, L., 2000. Simultaneous analysis of metabolites in potato tuber by gas chromatography–mass spectrometry. Plant J. 23, 131–142.

Sato, S., Soga, T., Nishioka, T., Tomita, M., 2004. Simultaneous determination of the main metabolites in rice leaves using capillary electrophoresis mass spectrometry and capillary electrophoresis diode array detection. Plant J. 40, 151–163.

Sauer, U., Hatzimanikatis, V., Bailey, J.E., Hochuli, M., Szyperski, T., Wuthrich, K., 1997. Metabolic fluxes in riboflavin-producing *Bacillus subtilis*. Nat. Biotechnol. 15, 448–452.

Schaefer, U., Boos, W., Takors, R., Weuster-Botz, D., 1999. Automated sampling device for monitoring intracellular metabolite dynamics. Anal. Biochem. 270, 88–96.

Schaub, J., Schiesling, C., Reuss, M., Dauner, M., 2006. Integrated sampling procedure for metabolome analysis. Biotechnol. Prog. 22, 1434–1442.

Schwender, J., Goffman, F., Ohlrogge, J.B., Shachar-Hill, Y., 2004. Rubisco without the Calvin cycle improves the carbon efficiency of developing green seeds. Nature 432, 779–782.

Shastri, A.A., Morgan, J.A., 2005. Flux balance analysis of photoautotrophic metabolism. Biotechnol. Prog. 21, 1617–1626.

Soga, T., Ueno, Y., Naraoka, H., Ohashi, Y., Tomita, M., Nishioka, T., 2002. Simultaneous determination of anionic intermediates for *Bacillus subtilis* metabolic pathways by capillary electrophoresis electrospray ionization mass spectrometry. Anal. Chem. 74, 2233–2239.

Sriram, G., Fulton, D.B., Iyer, V.V., Peterson, J.M., Zhou, R.L., Westgate, M.E., Spalding, M.H., Shanks, J.V., 2004. Quantification of compartmented metabolic fluxes in developing soybean embryos by employing biosynthetic ally directed fractional ^{13}C-labeling, [^{13}C, ^{1}H] two-dimensional nuclear magnetic resonance, and comprehensive isotopomer balancing. Plant Physiol. 136, 3043–3057.

Stephanopoulos, G., Aristidou, A.A., Nielsen, J., 1998. Metabolic Engineering Principles and Methodology. Academic Press, San Diego.

Sweetlove, L.J., Last, R.L., Fernie, A.R., 2003. Predictive metabolic engineering: a goal for systems biology. Plant Physiol. 132, 420–425.

Szyperski, T., 1998. ^{13}C NMR, MS and metabolic flux balancing in biotechnology research. Q. Rev. Biophys. 31, 41–106.

Theobald, U., Mailinger, W., Reuss, M., Rizzi, M., 1993. In vivo analysis of glucose-induced fast changes in yeast adenine-nucleotide pool applying a rapid sampling technique. Anal. Biochem. 214, 31–37.

van Dam, J.C., Eman, M.R., Frank, J., Lange, H.C., van Dedem, G.W.K., Heijnen, S.J., 2002. Analysis of glycolytic intermediates in *Saccharomyces cerevisiae* using anion exchange chromatography and electrospray ionization with tandem mass spectrometric detection. Anal. Chim. Acta 460, 209–218.

Van Dien, S.J., Strovas, T., Lidstrom, M.E., 2003. Quantification of central metabolic fluxes in the facultative methylotroph *Methylobacterium extorquens* AM1 using ^{13}C-label tracing and mass spectrometry. Biotechnol. Bioeng. 84, 45–55.

van Winden, W.A., van Dam, J.C., Ras, C., Kleijn, R.J., Vinke, J.L., van Gulik, W.M., Heijnen, J.J., 2005. Metabolic-flux analysis of *Saccharomyces cerevisiae* CEN.PK113-7D based on mass isotopomer measurements of ^{13}C-labeled primary metabolites. FEMS Yeast Res. 5, 559–568.

Villas-Boas, S.G., Hojer-Pedersen, J., Akesson, M., Smedsgaard, J., Nielsen, J., 2005. Global metabolite analysis of yeast: evaluation of sample preparation methods. Yeast 22, 1155–1169.

Visser, D., van Zuylen, G.A., van Dam, J.C., Oudshoorn, A., Eman, M.R., Ras, C., van Gulik, W.M., Frank, J., van Dedem, G.W.K., Heijnen, J.J., 2002. Rapid sampling for analysis of in vivo kinetics using the BioScope: a system for continuous-pulse experiments. Biotechnol. Bioeng. 79, 674–681.

Wiechert, W., Mollney, M., Isermann, N., Wurzel, W., de Graaf, A.A., 1999. Bidirectional reaction steps in metabolic networks: III. Explicit solution and analysis of isotopomer labeling systems. Biotechnol. Bioeng. 66, 69–85.

Wiechert, W., Mollney, M., Petersen, S., de Graaf, A.A., 2001. A universal framework for ^{13}C metabolic flux analysis. Metabol. Eng. 3, 265–283.

Wiechert, W., Siefke, C., de Graaf, A.A., Marx, A., 1997. Bidirectional reaction steps in metabolic networks: II. Flux estimation and statistical analysis. Biotechnol. Bioeng. 55, 118–135.

Wittmann, C., Kromer, J.O., Kiefer, P., Binz, T., Heinzle, E., 2004. Impact of the cold shock phenomenon on quantification of intracellular metabolites in bacteria. Anal. Biochem. 327, 135–139.

Yang, C., Hua, Q., Shimizu, K., 2002. Metabolic flux analysis in *Synechocystis* using isotope distribution from ^{13}C-labeled glucose. Metabol. Eng. 4, 202–216.

Zhao, J., Baba, T., Mori, H., Shimizu, K., 2004. Global metabolic response of *Escherichia coli* to gnd or zwf gene-knockout, based on ^{13}C-labeling experiments and the measurement of enzyme activities. Appl. Microbiol. Biotechnol. 64, 91–98.

Zhao, J., Shimizu, K., 2003. Metabolic flux analysis of *Escherichia coli* K12 grown on ^{13}C-labeled acetate and glucose using GG–MS and powerful flux calculation method. J. Biotechnol. 101, 101–117.